

Structural, magnetic and x-ray absorption studies of $\text{NdCo}_{1-x}\text{Ni}_x\text{O}_3$ ($0 \leq x \leq 0.5$)

Vinod Kumar^{1a}), Yogesh Kumar², Rajesh Kumar¹, D.K.Shukla³, S.K.Arora⁴, I.V.Shvets⁴ and Ravi Kumar⁵

¹*Department of Physics, National Institute of Technology, Hamirpur (H.P) – 177 005, India.*

²*Pohang Accelerator Laboratory, Pohang University of Science and Technology, Pohang 790-784, Republic of Korea.*

³*Deutsches Elektronen-Synchrotron DESY, 22607 Hamburg, Germany.*

⁴*CRANN, School of Physics, Trinity College Dublin, Dublin 2, Republic of Ireland.*

⁵*Centre for Materials Science & Engineering, National Institute of Technology, Hamirpur (H.P) 177 005, India.*

We have systematically investigated the effect of Ni substitution on the structural and magnetic properties of NdCoO_3 . Single phase nature and orthorhombic $Pbnm$ structure is confirmed by the Reitveld refinement of X-ray diffraction data in all samples. X-ray absorption near edge spectroscopy of Co and Ni K-edges reveal the presence of trivalent state of Ni and Co ions in all samples. Composition dependent crossover from canted antiferromagnetic (AFM) (for $x < 0.3$) to spin glass behavior (for $x \geq 0.3$) is observed in magnetic measurements. Low temperature ferromagnetic (FM) component in doped samples is attributed to the stabilization of Co^{+3} ions in IS spin state. The FM and AFM are observed to coexist as confirmed by M-H hysteresis. Nd sublattice seems to inhibit the magnetic contribution from Co ions and we ruled out the possibility of charge disproportion induced by Ni substitution leading to FM interactions in these systems as proposed in different reports.

^aElectronic mail: kumarvinodphy@gmail.com

I. INTRODUCTION

Perovskite oxides of $3d$ Co metal of type $R\text{CoO}_3$ with R as a rare-earth element are of particular interest primarily due to the presence of Co^{+3} ion exhibiting various spin-states. It provides an extra degree of freedom in addition to the charge, orbital and lattice degrees of freedom. The first member of this family (LaCoO_3) has been intensively studied and debated for different controversies for more than five decades¹⁻⁶. As a result of comparable Hund's exchange energy E_{ex} and the crystal field splitting Δ_{cf} , $3d^6$ configuration of Co^{+3} ions in LaCoO_3 assumes flexibility in spin-states which can result in different spin states *viz.* nonmagnetic low-spin state $t_{2g}^6 e_g^0$ with $S = 0$ (LS), an intermediate-spin state $t_{2g}^5 e_g^1$ with $S = 1$ (IS) and a high-spin state $t_{2g}^4 e_g^2$ with $S = 2$ (HS). In $R\text{CoO}_3$ family, LaCoO_3 exists in rhombohedral structure and all other members exhibit orthorhombic structure.

In addition to this extra spin-state degree of freedom the substituted cobaltites $R_{1-x}\text{A}_x\text{CoO}_3$ ($A =$ alkali earth metal) have also received considerable attention because of other properties like phase competition between long-range ordered ferromagnetism (FM) and spin-glass (SG) or cluster-glass (CG) ground states⁷⁻¹¹. The cause of occurrence of the ferromagnetism in the metallic cobaltites and manganites remains the subject of discussions for a long time. Most studies suggest that trivalent and tetravalent Co ions coexist in mixed (LS and IS) spin state.¹² Also, it has been shown that the cause of FM coupling for mixed valence cobaltites is different than that for manganites¹³. For cobaltites the LDA+U calculation shows that IS state is energetically comparable to LS state, but much more stabilized than HS state due to larger Co-O, $d-p$ hybridization.¹⁴ The electronic configurations having e_g electron and t_{2g} hole ($t_{2g}^5 e_g^1$, $t_{2g}^4 e_g^1$) are termed as IS states, and the degree of freedom to occupy one of the two fold-degenerate e_g orbitals gives rise to interesting physical properties, such as Jahn-Teller effect, orbital ordering, metallicity, and ferromagnetism. In addition to SrCoO_3 , compounds having Co ions, such as $\text{SrFe}_{1-x}\text{Co}_x\text{O}_3$, $\text{Sr}_{1-x}\text{La}_x\text{CoO}_3$, and $\text{LaCo}_{1-x}\text{Ni}_x\text{O}_3$, show

metallicity and ferromagnetism for certain compositions.¹⁵⁻²⁰ However the origin of magnetic interactions in these oxides is not yet clear and well understood as compared to manganites; especially the ferromagnetism in compounds containing Ni and Co lacks clear explanations.

RMO_3 is an interesting system to study the magnetic interactions between rare earth ion and 3d transition metal ions (M). Among RMO_3 , $NdMO_3$ family has been studied extensively with various magnetic and non-magnetic metal ions. A rich behavior can also emerge from the substitution at M site, which may give rise to greater disorder in comparison to the substitution at R site.²¹ If M is a 3d magnetic ion such as Fe, Ni or Cr, the M–M interaction orders antiferromagnetically with a small canting angle at high temperatures. At low temperature M–Nd exchange interactions give rise to spin reorientation of the M sublattice as shown by Parra-Borderias *et al.*²² The antiferromagnetic (AFM) ordering between Nd and M sublattices sometimes remains uncompensated where FM/ AFM order of M sublattice creates an onsite effective field, leading to polarization of Nd sublattice. Such polarization has been observed by neutron diffraction at low temperature.^{23, 24} In particular $NdCoO_3$ is a semiconductor exhibiting change in the activation energy with temperature which further coincides with the partial transformation of cobalt from LS (Co^{+3}) to HS(Co^{+3}) state.²⁵ On the other hand $NdNiO_3$ exhibit temperature driven metal insulator transition along with antiferromagnetic ordering²⁶. The Ni substitution in RMO_3 fetches our attention due to significant changes it brings in the properties of the systems. The magnetic behavior of mixed perovskites ($RNi_{1-x}Co_xO_3$) has been studied by several groups such as $LaNi_{1-x}Co_xO_3$ shows metallic behavior below room temperature up to $x = 0.6$ and semiconducting behavior for higher Co content.²⁷⁻³⁰ Recent studies of our group has reported many fascinating aspects in Ni-doped $RFeO_3$ compounds regarding the semiconducting ferromagnetic behavior, stabilization of magnetic structure by reducing the asymmetry in hysteresis and spin reorientation phenomena.^{31, 32, 33} The $LaNi_xCo_{1-x}O_3$ series have been observed to exhibit a

variety of interesting physical phenomena such as giant negative magneto resistance for $x \leq 0.35$ and metallic conductivity for $x > 0.35$, disorder induced metal insulator transitions, reentrant spin glass behavior and ferromagnetism.^{28, 34-35}

All these reports in literature regarding different issues motivate us to study $R\text{CoO}_3$ system with nickel substitution particularly in NdCoO_3 due to the fascinating properties exhibited by compounds containing Nd as mentioned above. Moreover there are a few findings on Ni substitution in $R\text{CoO}_3$ system and most of them are limited to LaCoO_3 with nonmagnetic sublattice of La only. However Nd being magnetic sublattice will provide an opportunity to see its effect on the magnetic properties of the system as a whole, which has not been possible in LaCoO_3 . In addition to this the effect of $d-d$ interactions between transition metal networks on the system can also be investigated.

In the present study, we have investigated the effect of Ni substitution on structural, magnetic and electronic structure of NdCoO_3 .

II. EXPERIMENTAL DETAILS

The single phase $\text{NdCo}_{1-x}\text{Ni}_x\text{O}_3$ ($0 \leq x \leq 0.5$) samples were prepared by conventional solid state reaction method. Stoichiometric amounts of Nd_2O_3 , NiO , and Co_3O_4 with purity not less than 99.95 % (Sigma Aldrich) were properly mixed and ground and then calcined at 900 °C. This process is repeated for two times. Finally, calcined powder was further ground and pressed into pellets and sintered at 1200 °C. Room temperature x-ray diffraction measurements were performed using PANalytical X'Pert PRO x-ray diffractometer having Cu-K_α source. The dc magnetization measurements including magnetic hysteresis loop and temperature dependent magnetization with zero field cooling (ZFC), field cooled cooling (FCC) and field cooled warming (FCW) processes were performed using Physical properties measurement system (PPMS) of Quantum design. The ac-susceptibility (χ) was measured in an ac field of 15Oe at frequencies of 1.3, 13, 133, and 1333 Hz, using SQUID magnetometer

(Quantum Design). The x-ray absorption studies of Co and Ni K- edges have also been performed at C beam line of the DORIS III storage ring (DESY, Hamburg, Germany). Spectra at Ni K-edge were collected in both fluorescence and transmission modes while that for Co was collected only in transmission mode. All the spectra were collected at liquid N₂ temperature with temperature stability of 1K and 0.1 K at 300K and 77 K, respectively.

III. RESULTS AND DISCUSSION

A. Structural Analysis

To determine the crystal structure and single phase nature of prepared samples, room temperature powder x-ray diffraction studies of NdCo_{1-x}Ni_xO₃ ($0 \leq x \leq 0.5$) were performed. The obtained XRD patterns were analyzed with Reitveld refinement using FULLPROF Code. Figure 1 shows the XRD patterns of samples along with the fitted curves and difference line. The analysis of data suggests that all the samples exhibit single phase orthorhombic structure with space group *Pbnm*. However for a Ni concentration $x = 0.5$ the line width and intensity difference of various reflections is increased indicating small distortion in the structure. In NdCo_{1-x}Ni_xO₃ ($0 \leq x \leq 0.5$), Nd is associated with Wyckoff position (4*c*) ($x, y, 1/4$), Co/Ni is at position 4*b* ($1/2, 0, 0$), O1 is at 4*c* ($x, y, 1/2$) and O2 is at 8*d* (x, y, z). The calculated parameters are given in Table I. The lattice parameters increased linearly with the increase in Ni concentration and hence unit cell volume is also increased, which confirms that Co ions replaced by Ni in NdCoO₃ lattice either as Ni⁺² or Ni⁺³ since the ionic radii ($r(\text{Ni}^{+2}) > r(\text{Ni}^{+3}) > r(\text{Co}^{+3}) \approx r(\text{Co}^{+4})$).³⁵

B. X-ray absorption studies

In order to determine the valence state of Co and Ni, we performed x-ray absorption near edge spectroscopy (XANES) of Co and Ni K-edge for all the samples. Figure 2 shows Co K-edge XAS curve for NdCo_{1-x}Ni_xO₃ ($0 \leq x \leq 0.5$). The energy is calibrated by Co metal foil. The edge energy (E_0) for all the doped samples is similar and lie higher than those of standard

samples Co, CoO (Co⁺²), and close to Co₂O₃ (Co⁺³) (as marked in Fig. 2), which indicates that the compositions are having Co in trivalent state.³⁶ From Fig. 3 we observe that Ni absorption edge of all the doped samples is close to that of Ni⁺³.^{37, 38} Moreover a pre-edge structure in Co K-edge, lying below 7715eV has been observed and is shown in inset to Fig 2. In previous investigations this has been assigned to Co⁺³ 1s -3d transitions³⁶ and was suggested due to two contributions. A low-energy feature marked ‘A’ in inset to Fig.2 is attributed to transitions to the *t_{2g}* orbitals, and another marked as ‘B’ at higher energy attributed to the *e_g* orbitals. The relative change of their spectral weight with Ni substitution is therefore a signature of *t_{2g}*→*e_g* electron transfer *i.e.* a transition to excited spin states predominantly to IS state.³⁹ Thus the X-ray absorption results suggest that both Co and Ni are in +3 state and a continuous LS to IS state transition of Co with Ni substitution.

C. Magnetization Studies

Figure 4(a-f) shows the magnetization as a function of temperature. From Fig.4 it is clearly observed that the magnetic susceptibility is increased below 50K for all samples, which indicate the possibility of ferromagnetic (FM) coupling. But the negative Weiss constant (θ) calculated by fitting the magnetic susceptibility data to Curie Weiss law $\chi = C/T - \theta$ at temperature above 100 K (see Table II) suggests presence AFM interactions. It may be due to the presence of the canted AFM ordering, which can give rise to a weak FM response⁴⁰. The anti-parallel alignment of Nd moments to the Co sublattice may give rise to such AFM ordering, which is already seen in compounds based on Co and Nd.^{11,41-43} The contribution from magnetic interactions among Co ions appear to be hindered by the presence of the magnetic moment of Nd. It may also be the reason for the observed mismatch between the values of magnetic moment (Table II) calculated from measured data and the one predicted using simple ionic model. This mismatch may also be accounted due to the presence of significant Co-O hybridisation occurring in cobaltites.⁴⁴

Now for the compositions $x \geq 0.3$, we observe that ZFC curve passes through a maximum and then fall sharply with the decreasing temperature. Furthermore, ZFC and FC curves bifurcate at a temperature greater than the one at which the maximum occurs, thus shows the signature of typical spin glass (SG) behaviour. The assertion of spin glass behaviour for $x \geq 0.3$ is further supported by the shift of peak at T_f (spin glass freezing temperature) observed in *ac* susceptibility (χ'_{ac}) towards higher temperature with increase in frequency (see Fig. 5). Below T_f , χ'_{ac} shows frequency dependence and above this it becomes independent of frequency, which is a feature of conventional spin glasses.⁴⁵ Such behaviour is already reported for similar systems.^{7, 17, 46-49} In these reports a competing FM-AFM interactions are supposed to give rise to glassy magnetic behaviour. In our case AFM interaction can be either due to AFM alignment of the magnetic moments of Nd and Co or due to the super exchange interactions between Co^{+3} or Ni^{+3} ions. However, this behaviour is observed only after a certain level of Ni substitution, which may be attributed to the enhancement of AFM interactions between the ions of same valences with increased Ni concentration.

In contrast to AFM, the origin of FM component in systems containing Ni and Co is very complex. In earlier studies Perez *et al.*²⁰ proposed two possible mechanisms for the FM ordering: first a change in the spin state of Co due to the presence of Ni and second due to charge transfer of the type $\text{Ni}^{+3} + \text{Co}^{+3} \Leftrightarrow \text{Ni}^{+2} + \text{Co}^{+4}$ giving rise to $\text{Co}^{+3} - \text{O} - \text{Co}^{+4}$ double exchange interactions. Hammer *et al.*³⁴ also quoted these in their work but were unable to distinguish between these in their findings. Since our XANES results clearly show that both Co and Ni ions are in trivalent state, we rule out the possibility of charge disproportionation in the present system. Similar findings have also been reported by T. Kyômen *et al.*⁵¹ on $\text{LaCo}_{0.5}\text{Ni}_{0.5}\text{O}_3$, in which they discarded charge transfer and suggested increase in population

of Co e_g . So our results seem to be consistent with mechanism of change in spin state and the cause of FM at low temperature can be understood in present investigation as follows.

Since, with the Ni substitution lattice parameters increase (*i.e.* lattice expands) leading to a decrease in Δ_{cf} , more population of Co ions in IS state is favoured. This is consistent with the earlier investigations⁵¹ of controlling the spin state of cobalt by chemical substitution and is also supported by our XAS data discussed in the previous section. So, it is apparent that Ni substitution provides expanded lattice and stabilize some pairs of Co ion in IS state even down to low temperature, which is not seen in pure compound, where at low temperatures IS to LS transition takes place.⁵² In IS state cobalt has e_g^1 orbital configuration and these orbitals, if ordered will give rise to ferromagnetic interactions between IS Co^{+3} ions.^{14, 51, 52} This continuous evolution of FM component can also be inferred from the value of Weiss constant (Table II), which becomes less negative with increase in Ni substitution. So as the Ni content increases, more pairs of cobalt ions get stabilized in IS state keeping Ni in LS. When it reaches a critical value $x = 0.3$, the FM interactions between these IS Co^{+3} ions compete with the AFM interactions between $\text{Ni}^{+3} - \text{O} - \text{Ni}^{+3}$ and a fraction of LS $\text{Co}^{+3} - \text{O} - \text{LS} \text{Co}^{+3}$ and give rise to magnetic frustration.

The rise in magnetic frustration with Ni substitution is also evident from Fig.4(d-f), where an increase in the separation between ZFC and FC curves has been observed as we go from $x = 0.3$ to $x = 0.5$. In Fig. 6, M-H curves obtained at 10 K are shown, where a small nonlinear component starts to appear at $x = 0.2$. But for compositions $x \geq 0.3$, curves clearly show a minor hysteresis at small fields and at higher fields M varies linearly with H showing a typical AFM response.

Therefore, from above discussion we conclude the coexistence of competing FM and AFM components leading to glassy behaviour at low temperature.

A different behaviour of FC curve is observed for $x=0.5$ composition. It can be attributed to structural disorder, which can also contribute to magnetic disorder. As lattice parameters change with Ni substitution, significant distortions in lattice are induced for $x = 0.5$ as described in Section III A. The magnetic interactions are dependent on the bond angles (M-O-M) and bond lengths, therefore any change in these parameters will affect the nature as well as the overall magnitude of the magnetic interactions. Furthermore Co^{+3} (IS) and Ni^{+3} (LS) have similar population in e_g orbitals, which may render similar size to these ions giving rise to disordered arrangement of Ni and Co ions over a large scale.⁵³ This will also account for the increased magnetic disorder observed at higher Ni substitution.

Thus, the overall magnetic behaviour can be explained on the basis of simultaneous presence of different magnetic phases, where one phase evolves at the expense of other. This evolution is due to a change in the character of magnetic interactions which are sensitive to temperature and structural disorder as well as to the changes in spin state of cobalt induced by Ni substitution.

IV. CONCLUSION

The structural, magnetic, and electronic structure have been systematically investigated for $\text{NdCo}_{1-x}\text{Ni}_x\text{O}_3$ in the substitution range of $0 \leq x \leq 0.5$. The X-ray diffraction followed by Reitveld analysis confirms that all the specimens exhibit orthorhombically distorted perovskite structure with space group $Pbnm$. The unit cell parameters and volume at room temperature were found to gradually increase with Ni content, which is consistent with the differences in ionic radii of Co and Ni. The magnetic behaviour is found to be strongly dependent on the extent of substitution. The compounds with $x < 0.3$ exhibit transition from paramagnetic to AFM like behaviour down to low temperature, but compounds with $x \geq 0.3$ show spin glass behaviour in the same temperature range. Our results ruled out the possibility

of charge disproportion induced by Ni substitution leading to FM interactions in these systems as proposed in different reports. With our findings we propose stabilization of cobalt in IS state with the Ni substitution. The FM interactions between IS Co^{+3} ions then frustrate the AFM interactions between the ions of similar valences, which give rise to spin glass behaviour observed in the present system. Nd sublattice seems to mask the magnetic ordering of Co ions. The possibility of structural or chemical disorder, which further has been related to the transition to IS state responsible for the magnetic disorder has also been not ruled out in present investigation. It is to be pointed out that substitution concentration $x \approx 0.3$ seems to be the threshold for concentration dependent changes in magnetism.

We finally conclude that Ni substitution in NdCoO_3 induces changes in crystal and electronic structure and it leads to frustration in the magnetic order of the system.

Acknowledgement:

The authors would like to thank Roman Chernikov for the help during the XAS measurements.

REFERENCES

- ¹G. H. Jonker and V. H. Van Santen, *Physica (Amsterdam)* **19**, 120 (1953).
- ²J. B. Goodenough and P. M. Raccah, *J. Appl. Phys.* **36**, 1031 (1965).
- ³M. A. Senaris-Rodriguez and J. B. Goodenough, *J. Solid State Chem.* **116**, 224 (1995).
- ⁴T. Saitoh, T. Mizokawa, A. Fujimori, M. Abbate, Y. Takeda and M. Takano, *Phys. Rev. B* **55**, 4257 (1997).
- ⁵S. Yamaguchi, Y. Okimoto and Y. Tokura, *Phys. Rev. B* **55**, R8666 (1997).
- ⁶Y. Kobayashi, N. Fujiwara, S. Murata, K. Asai and H. Yasuoka, *Phys. Rev. B* **62**, 410 (2000).
- ⁷M. A. Senaris-Rodriguez and J. B. Goodenough, *J. Solid State Chem.* **118**, 323 (1995).
- ⁸S. Mukherjee, R. Ranganathan, P. S. Anilkumar, and P. A. Joy, *Phys. Rev. B* **54**, 9267 (1996).
- ⁹M. Itoh, I. Natori, S. Kubota, and K. Motoya, *J. Magn. Magn.Mater.* **140**, 1811 (1995).
- ¹⁰A. K. Kundu, *Journal of Solid State Chemistry* **179**, 923 (2006).
- ¹¹D. D. Stauffer and C. Leighton, *Phys. Rev. B* **70**, 214414 (2004).
- ¹²P.M. Raccah and J.B. Goodenough, *Phys. Rev.B* **155**, 932 (1967).
- ¹³A .P. Sazonov, I.O. Troyanchuk, V.V. Sikolenko, G.M. Chobot, H. Szymczak, *J. Phys. Condens. Matter.* **17**, 4181 (2005).
- ¹⁴M. A. Korotin, S. Yu. Ezhov, I. V. Solovyev and V. I. Anisimov, *Phys. Rev. B* **54**, 5309 (1996).
- ¹⁵R.H. Potze, G.A. Sawatzky and M. Abbate, *Phys. Rev. B* **51**, 11501 (1995).
- ¹⁶M. Abbate, G. Zampieri, J. Okamoto, A. Fujimori, S. Kawasaki and M. Takano, *Phys. Rev. B* **65**, 165120 (2002).
- ¹⁷M. Itoh, I. Natori, I. Kubota and M. Motoya, *J. Phys. Soc. Jpn.***63**, 1486 (1994).
- ¹⁸S. Tsubouchi, T. Kyo men and M. Itoh, *Phys. Rev. B* **67**, 094437 (2003).

- ¹⁹K. Asai, H. Sekizawa, K. Mizushima, and S. Iida, *J. Phys. Soc.Jpn.* **43**, 1093 (1977).
- ²⁰J. Pe´rez, J. Garcí´a, J. Blasco, and J. Stankiewicz, *Phys. Rev. Lett.* **80**, 2401 (1998).
- ²¹ D. D. Sarma, A. Chainani, S. R. Krishnakumar, E. Vescovo, C. Carbone, W. Eberhardt, O. Rader, Ch. Jung, Ch. Hellwig, W. Gudat, H. Srikanth and A. K. Raychaudhuri, *Phys. Rev. Lett.* **80**, 4004 (1998).
- ²² M .P. Borderías , F . Bartolomé , J.A .Velamazán , J . Bartolomé_ *J. Phys: Condens. Matter* **23**, 046003 (2011).
- ²³P.Pataud and J. Sivardire, *J. Phys. France* **31**, 803-809 (1970).
- ²⁴I. Sosnowska and P. Fischer, *Phase Trans.* **8**, 319 (1987).
- ²⁵D. S. Rajoria, V. G. Bhide, G. Rama Rao and C. N. R Rao, *J.C.S. Faraday H* **70**, 512 (1974).
- ²⁶J. Garcia, L. Mufloz, J. Rodrfiguez-Carvaja and P. Lacorre, *Europhys. Lett.* **20** (3), 241 (1992).
- ²⁷J. Blasco and J. Garcí´a, *J. Phys. Chem. Solids* **55**, 843 (1994).
- ²⁸A. K. Raychaudhuri, *Adv. Phys.* **44**, 21 (1995).
- ²⁹K. P. Rajeev and A. K. Raychaudhuri, *Phys. Rev. B* **46**, 1309 (1992).
- ³⁰J. Blasco and J. Garcí´a, *Phys. Rev. B* **51**, 3569 (1995).
- ³¹R. Kumar, R. J. Choudhary, M. W. Khan, J. P. Srivastava, C. W. Bao, H. M. Tsai, J. W. Chiou, K. Asokan and W. F. Pong, *J. Appl. Phys.* **97**, 093526 (2005).
- ³²R. Kumar, R. J. Choudhary, M. Ikram, D. K. Shukla, S. Mollah, P. Thakur, K. H. Chae, B. Angadi and W. K. Choi, *J. Appl.Phys.* **102**, 073707 (2007).
- ³³A. Bashir, M. Ikram , R. Kumar, P. Thakur, K. H. Chae, W. K. Choi and V. R. Reddy, *J. Phys. Condens. Matter* **21**, 325501(2009).
- ³⁴D. Hammer, J. Wu and C. Leighton, *Phys. Rev. B* **69**, 134407 (2004).
- ³⁵T. Wu, G. Wu, X.H. Chen, *Solid State Communications* **145**, 293 (2008).

- ³⁶ J.Y.Chang, B.N. Lin, Y.Y. Hsu, H.C. Ku, *Physica B* **329-333**, 826 (2003); O. Toulemonde, N. N. Guyen, F. Studer, *J. Solid State Chem.* **158**, 208–217 (2001); O. Haas, R.P.W.J. Struis, J.M. McBreen, *J. Solid State Chem.* **177**, 1000–1010 (2004)
- ³⁷ H.Yi. Lee, T. B.Wu, J. Fu. Lee, *J. Appl. Phys.* **80**, 2175 (1996).
- ³⁸ M. C. Sanchez, J. Garcia, J. Blasco, G. Subias and J.P.Cacho, *Phys. Rev. B* **65**, 144409 (2002).
- ³⁹ G. Vankó, J.P. Rueff, A. Mattila, Z. Németh and A. Shukla, *Phys.Rev. B* **73**, 024424 (2006).
- ⁴⁰ M. L. Lopez, M. A. Arillo, I. Alvarez-Serrano, P. Martín, E. Rodríguez, C. Pico, M. L. Veiga, *J. Mats. Chem. and Phys.* **120**, 387 (2010).
- ⁴¹ A. Krimmel, M. Reehuis, M. Paraskevopoulos, J. Hemberger and A. Loidl, *Phys. Rev. B* **64**, 224404 (2001).
- ⁴² M. Reehuis, P. J. Brown, W. Jeitschko, H. M. Moller, and T.Vomhof, *J. Phys. Chem. Solids* **54**, 469 (1993).
- ⁴³ M. Reehuis, B. Ouladdiaff, W. Jeitschko, T. Vomhof, B. Zimmer, and E. Ressouche, *J. Alloys Compd.* **261**, 1 (1997)
- ⁴⁴ P. Ravindran, H. Fjellvag, A. Kjekshus, P. Blaha, K. Schwarz and J. Luitz, *J. Appl. Phys.* **91**, 291 (2002).
- ⁴⁵ J. A. Mydosh, *Spin-Glasses: An Experimental Introduction* (Taylor and Francis, London, 1993).
- ⁴⁶ Yi Yun Yang, *Applied Physics Research* Vol. **2** (1) 103-107 (2010).
- ⁴⁷ J. Wu and C. Leighton, *Phys. Rev. B* **67**, 174408 (2003).
- ⁴⁸ R. Caciuffo, D. Rinaldi, G. Barucca, J. Mira, J. Rivas, M. A. Señarís-Rodríguez, P. G. Radaelli, D. Fiorani, J. B. Goodenough, *Phys. Rev. B* **59**, 1068 (1999).
- ⁴⁹ J. Androulakis, N. Katsarakis, Z. Viskadourakis and J. Giapintzakis. *J. Appl. Phys.* **93**, 5484 (2003).

⁵⁰T. Kyômen, R. Yamazaki and M. Itoh, Phys. Rev. B **68**, 104416 (2003).

⁵¹J Q Yan, J S Zhou, and J B Goodenough, Phys. Rev. B **70** 014402 (2004).

⁵²I. O Troyanchuk, D. V Karpinsky and R. Szymczak, Physics of the solid state. **48** (4), 722 (2006); I O Troyanchuk, D V Karpinsky and R Szymczak, Phys. Stat. Sol. (b) **242**, 6 R49-R51(2005).

⁵³ I. Fita , V. Markovich, D. Mogilyansky, R. Puzniak, A. Wisniewski, L. Titelman, L. Vradman, M. Herskowitz, V. N. Varyukhin and G. Gorodetsky, Phys. Rev. B **77**, 224421 (2008).

FIGURES CAPTIONS :

Figure 1. Reitveld refined X-ray diffraction patterns for the samples $\text{NdCo}_{1-x}\text{Ni}_x\text{O}_3$ ($0 \leq x \leq 0.5$). In each panel solid squares represent observed data, the line shows the calculated profile. The difference between the observed and the calculated pattern is shown at the bottom.

Figure 2. X-ray near edge absorption (XANES) spectra for Co *K*-edge of $\text{NdCo}_{1-x}\text{Ni}_x\text{O}_3$ ($0 \leq x \leq 0.5$). No edge shift is observed on substitution. The enlarged view of pre edge region is shown in inset. The arrows indicate the shift in the spectral response with substitution.

Figure 3. X-ray near edge absorption (XANES) spectra for Ni *K*-edge of $\text{NdCo}_{1-x}\text{Ni}_x\text{O}_3$ ($0 \leq x \leq 0.5$). Clear indication of +3 valance state of Ni appears in all composition.

Figure 4. Temperature dependence of *dc* magnetic susceptibility under different modes at a field of 1kOe for $\text{NdCo}_{1-x}\text{Ni}_x\text{O}_3$ ($0 \leq x \leq 0.5$). Solid squares represent zero-field cooling (ZFC), open circles show field cool cooling (FCC) and open triangles are for field cool warming (FCW) mode. A bifurcation in ZFC and FC curves appears after $x=0.2$ which shows a composition dependent magnetic behaviour at low temperature.

Figure 5. The variation of AC magnetic susceptibility with temperature at different frequencies for $x \geq 0.3$. T_f represents the spin glass freezing temperature. The shifting of peak position to higher temperature with increase in frequency is clearly seen

Figure 6. Isothermal Magnetization hysteresis loops (M-H) of $\text{NdCo}_{1-x}\text{Ni}_x\text{O}_3$ ($0 \leq x \leq 0.5$) at 10 K. Change in the shape of the plots with substitution indicates to the coexistence of AFM and FM ordering for samples with $x \geq 0.3$.

Table I. Reitveld refined unit cell parameters for $\text{NdCo}_{1-x}\text{Ni}_x\text{O}_3$ ($0 \leq x \leq 0.5$).

Name	a (Å)	b (Å)	c (Å)	V (Å ³)	χ^2
NdCoO_3	5.3503	5.3349	7.5513	215.54	1.17
$\text{NdCo}_{0.9}\text{Ni}_{0.1}\text{O}_3$	5.3554	5.3454	7.5608	216.44	1.85
$\text{NdCo}_{0.8}\text{Ni}_{0.2}\text{O}_3$	5.3582	5.3540	7.5734	217.26	1.21
$\text{NdCo}_{0.7}\text{Ni}_{0.3}\text{O}_3$	5.3777	5.3667	7.5865	218.94	1.37
$\text{NdCo}_{0.6}\text{Ni}_{0.4}\text{O}_3$	5.3778	5.3676	7.5870	218.99	1.38
$\text{NdCo}_{0.5}\text{Ni}_{0.5}\text{O}_3$	5.4481	5.3658	7.5912	221.92	1.97

Table II. Parameters *viz.* effective magnetic moment μ_{eff} and Weiss constant (θ) calculated for $\text{NdCo}_{1-x}\text{Ni}_x\text{O}_3$ ($0 \leq x \leq 0.5$) from Curie Weiss fit of magnetization data measured at 1000 Oe of applied field.

x	μ_{eff} (μ_B)	θ (K)
0	3.57	-88
0.1	3.28	-78
0.2	3.68	-67
0.3	3.70	-44
0.4	3.74	-40
0.5	3.89	-49

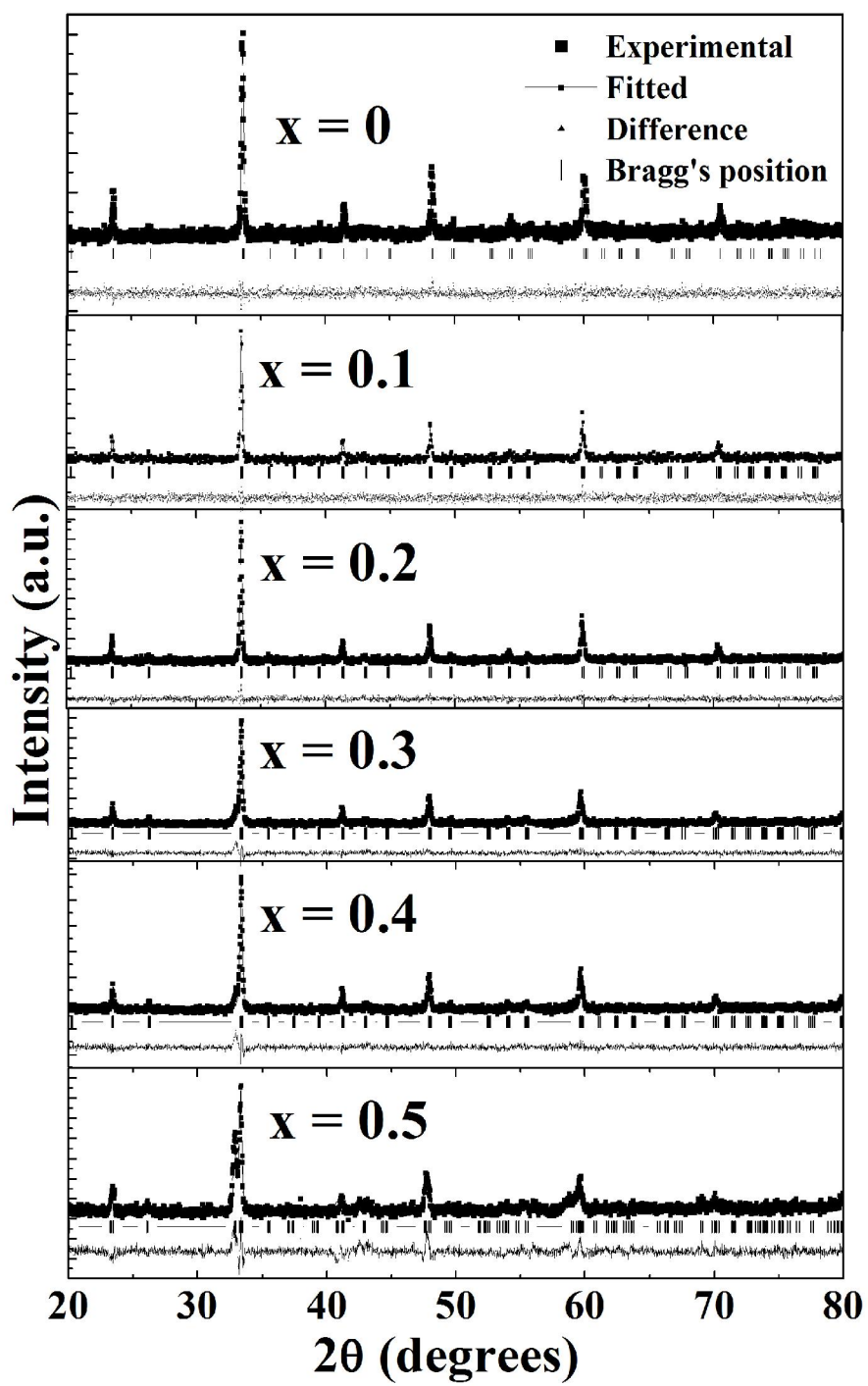


Fig.1

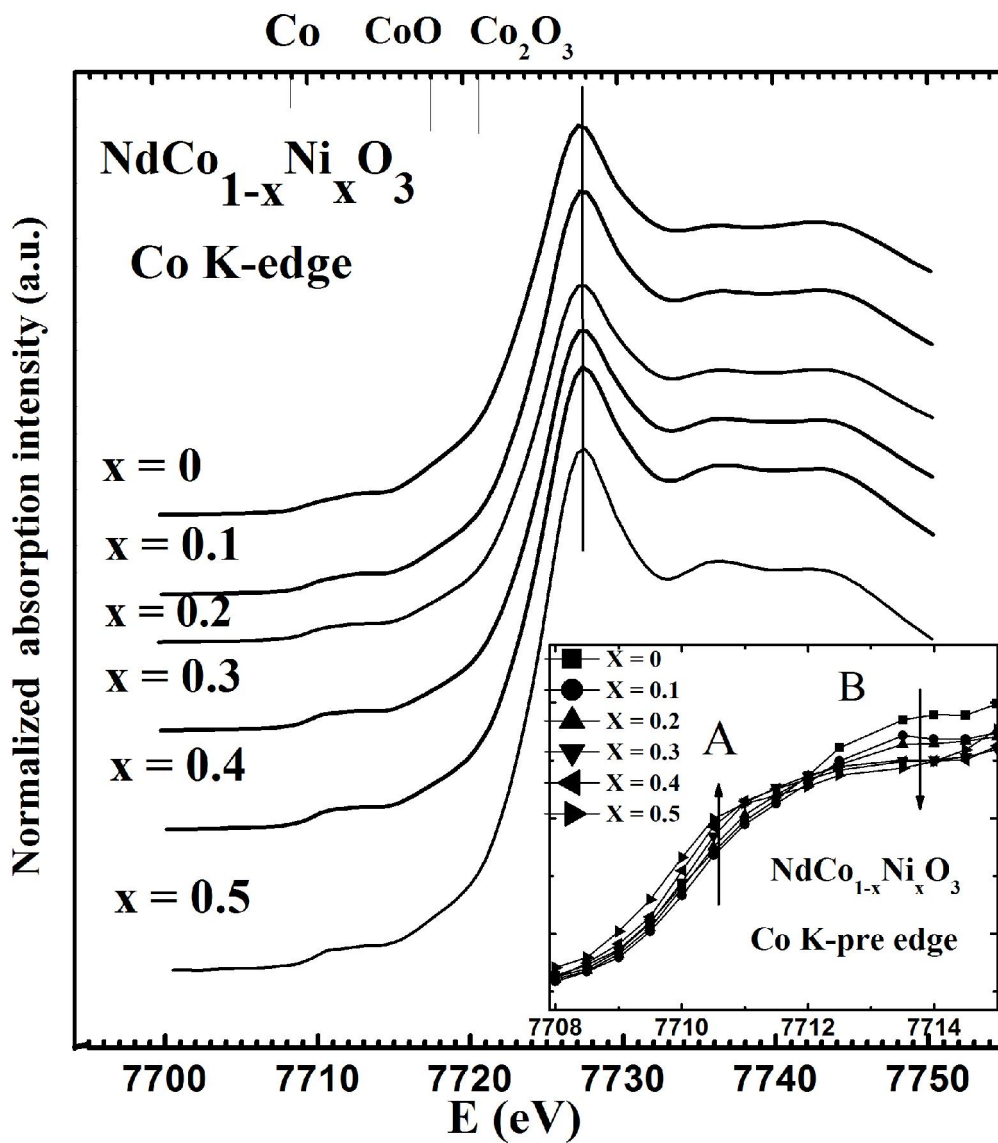


Fig.2

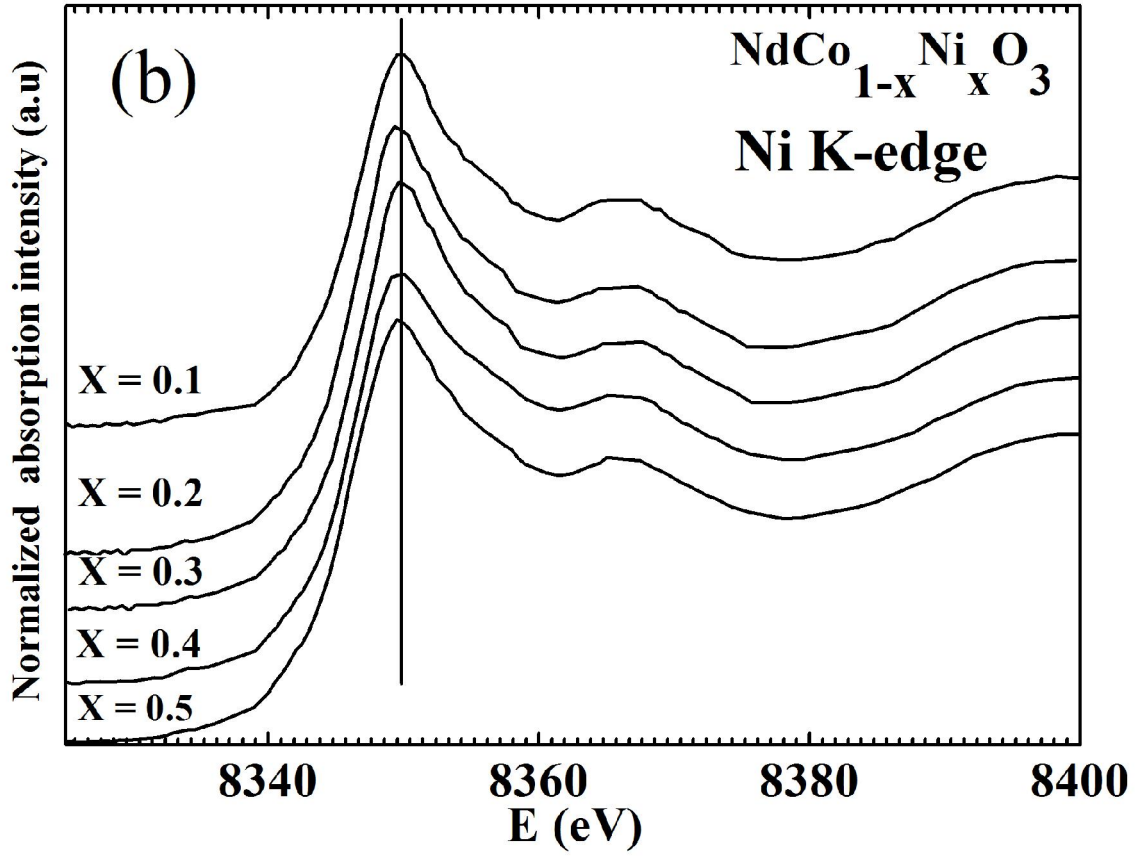


Fig.3

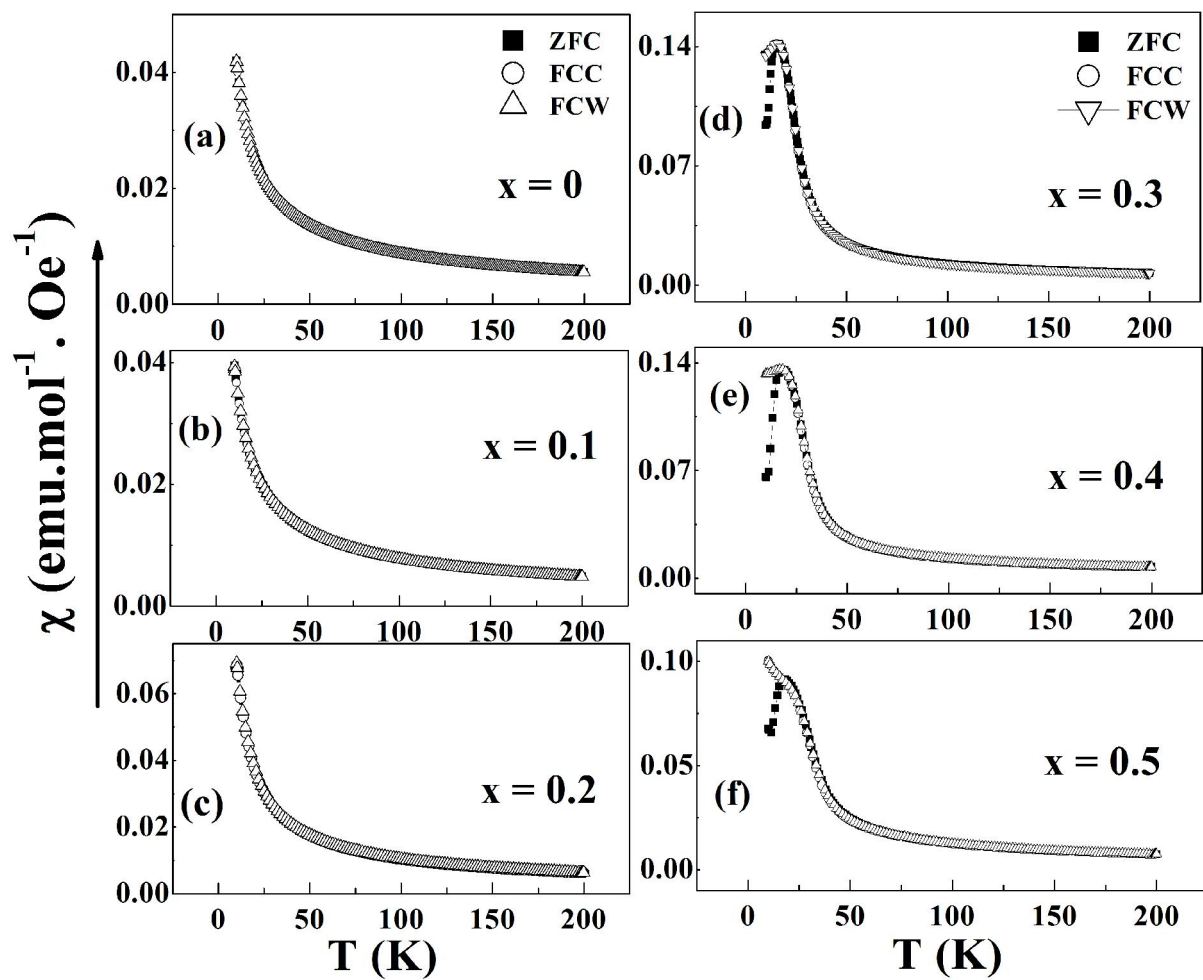


Fig.4

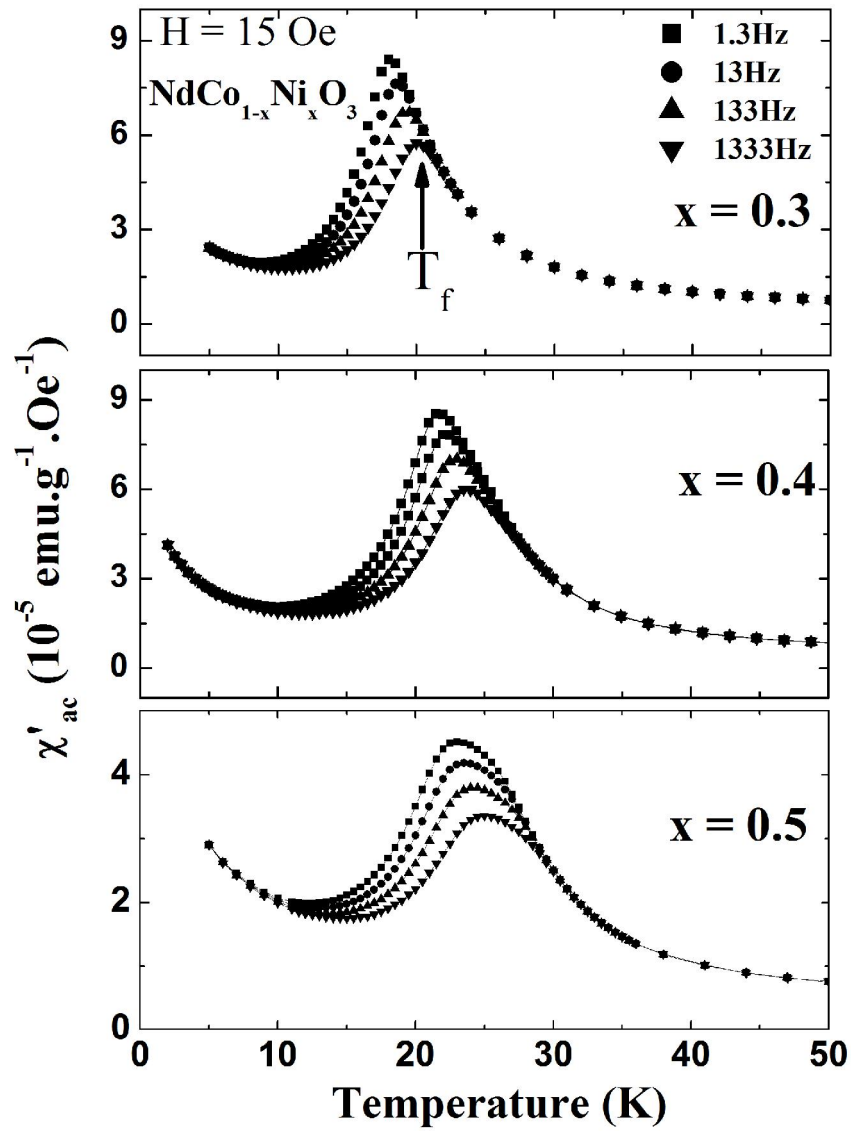


Fig.5

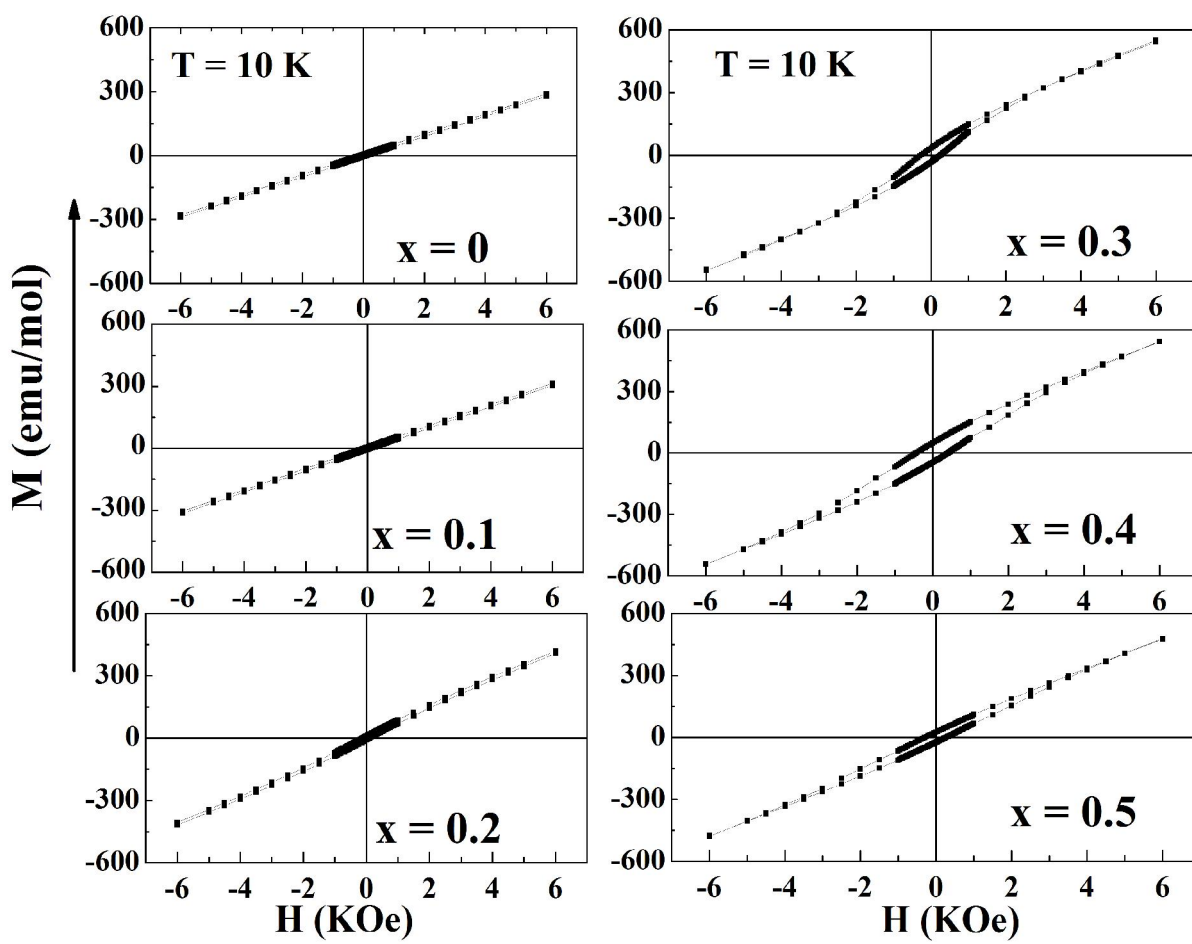


Fig.6